Chapter 8
Electrospun Fluorescent Nanofibers for Explosive Detection

Anitha Senthamizhan and Tamer Uyar

Abstract Development of an instant on-site visual detection method for 2,4,6 trinitrotoluene (TNT) has become a significant requirement of the hour towards a secured society and a greener environment. Despite momentous advances in the respective field, a portable and reliable method for quick and selective detection of TNT still poses a challenge to many reasons attributing to inappropriate usage in subordinate areas and untrained personnel. The recent effort on the fluorescent based detection represents as one of easy method in terms of fast response time and simple on/off detection. Therefore, this chapter provides a consolidation of information relating to recent advances in fluorescence based TNT detection. Further, the main focus will be towards advances in the nanofibers based TNT detection and their reason to improving the sensitivity.

8.1 Introduction

The last few decades has experienced extensive urbanization and industrialization, resulting in the extraordinary mobilization of natural resources, ultimately causing environmental pollution. The pollution caused by the harmful explosives 2,4,6 trinitrotoluene (TNT) has been regarded as a ruinous element, looked upon as a security threat. TNT has been listed on the United States Environmental Protection Agency (US EPA) priority pollutants: a known mutagen, causing pancytopenia as a result of bone marrow failure [1]. One of the striking features of these aromatic nitro compounds has been their resistance to chemical or biological oxidation and hydrolysis attributed to the presence of electron-withdrawing nitro groups present in them [2–4].

A. Senthamizhan
UNAM-National Nanotechnology Research Centre, Bilkent University, Ankara 06800, Turkey

T. Uyar (✉)
UNAM-National Nanotechnology Research Centre, Bilkent University, Ankara 06800, Turkey

Institute of Materials Science & Nanotechnology, Bilkent University, Ankara 06800, Turkey
e-mail: uyar@unam.bilkent.edu.tr

A. Macagnano et al. (eds.), *Electrospinning for High Performance Sensors*,
NanoScience and Technology, DOI 10.1007/978-3-319-14406-1_8

Subsequently, owing to their resistance, their treatment and remediation techniques pose a serious threat. In addition, TNT has a very low mobility once adsorbed into the soil. As set by the US EPA, the maximum allowable concentration of these compounds in drinking water are about 2 parts-per-billion (ppb) and a resident soil screening level of 19 milligrams per kilogram (mg/kg) and an industrial soil screening level of 79 mg/kg [5]. Keeping in mind the security and safety of the public and the environment, investigations of arson, post-blast residues and locating the buried land mines is the need of the hour. This has grabbed the attention and interest for the detection of nitroaromatic explosives in the recent years [6, 7]. Following the speculation and the need, numerous methods have been devised for the detection of TNT, namely gas and liquid chromatography, mass spectrometry, surface plasmon resonance (SPR), surface enhanced Raman scattering (SERS), field-effect transistors, electrochemical methods and fluorescent and colorimetric methods [8–12]. These techniques, however, suppose to be time consuming, requiring bulky equipment with a tedious way of preparing the sample and usually require an expert operator. Apart from these methods, biological methods such as bioreactors, bioslurry treatment, and passive subsurface biobarriers have been put into use for developing efficacious method in reducing TNT concentrations [3–6].

Further, most of the methods and systems have the disadvantage of not being able to be downsized, lacking the ability to be performed in an automated high-throughput analysis. This calls in for some improvement in the sensing techniques, attracting considerable research efforts in recent years. Among the various techniques, fluorescence-based sensors appear simple, cost-effective, and highly sensitive detection modalities [13–17]. Adding to the list, miniaturized smart sensors based on one-dimensional (1D) nanostructures have gained much attention owing to their fast and high sensitivity towards enhanced adsorption. The large surface-to-volume ratio and the high dispersivity of the nanostructured materials essentially provide a large surface area for the adsorption and thus the enrichment of the analyte. This also contributes to the stable immobilization of a large amount of molecular recognition elements, resulting in the excellent improvement of the sensitivity and selectivity of the sensor. Some such one-dimensional (1D) nanomaterials are, silicon nanowires, metal oxide nanowires and carbon nanotubes have been utilized to fabricate TNT sensors [18–23]. This chapter will oversee the recent advances in the development of various techniques and approaches designed for TNT sensors. Furthermore, we will concentrate on the usage of electrospun nanofibers for the improved TNT sensing performance.

8.2 Colorimetric Detection

Colorimetric technique has received much attention due to its short response time, excellent sensitivity, simplicity and most convenient to execute which highly suitable for real time application. Until now, there have been a variety of quantum

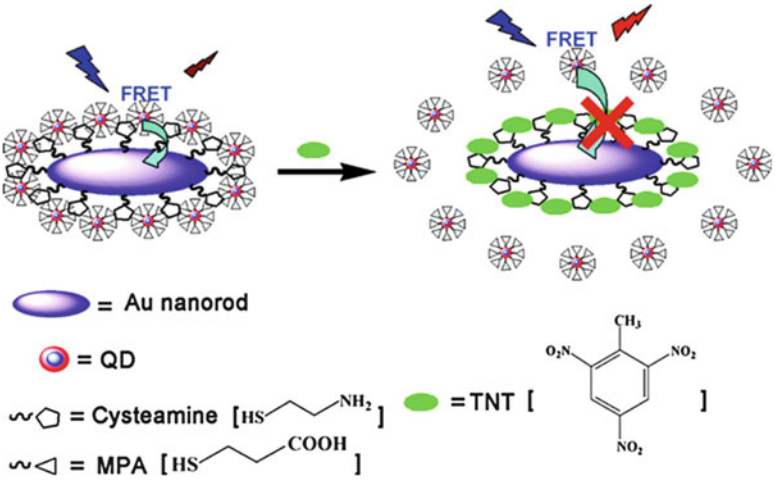

Fig. 8.1 Structure of the hybrid AuNR–QDs assembly and schematic illustration of FRET-based operating principle [24a]

dots used because of its size tunable emission spectrum and apparent improvement fluorescent dye molecules that they do not photobleach [15, 17, 19, 20]. The quenching processes are believed to occur via analyte induced aggregation or reversible electron transfer mechanism or chemical oxidation [21–23]. Recently Yunsheng Xia et al. designed turn-on fluorescent TNT sensor, consisting of gold nanorod (AuNR) and QDs for turn-on fluorescent sensing of TNT in near-infrared region [24a]. Further, they have modified with short thiol-molecules such as cysteamine and 3-mercaptopropionic acid (MPA), respectively to form hybrid assembly through amine-carboxyl attractive interaction. The reported design is shown in Fig. 8.1. In the presence of TNT, the preformed assembly gets broken because they can replace the QDs around AuNRs, based on the specific reaction of forming meisenheimer complexes between TNT and primary amines.

Thus, the forster resonance energy transfer (FRET) is switched off, and a more than 10 times fluorescent enhancement is obtained. The fluorescence turn-on is immediate, and the limit of detection for TNT is as low as 0.1 nM. Importantly, TNT can be well distinguished from its analogues due to their electron deficiency difference. Ellen R. Goldman demonstrated the self-assembled QD-based FRET sensor for the specific detection of the explosive TNT in aqueous environments [22]. The sensor consists of anti-TNT specific antibody fragments, appended with an oligohistidine sequence, specifically immobilized on the surface of Cadmium selenide- zinc sulfide (CdSe-ZnS) QDs. The use of an antibody fragment instead of a full antibody provides a more compact QD conjugate and is better suited for FRET, as distances between donor and antibody-bound acceptor are substantially reduced. The assembled conjugate produced a substantial rate of FRET when pre-assembled with a quencher-labeled TNT analogue. The unique optical properties of noble metal nanostructures have placed a vital role in the field of biological

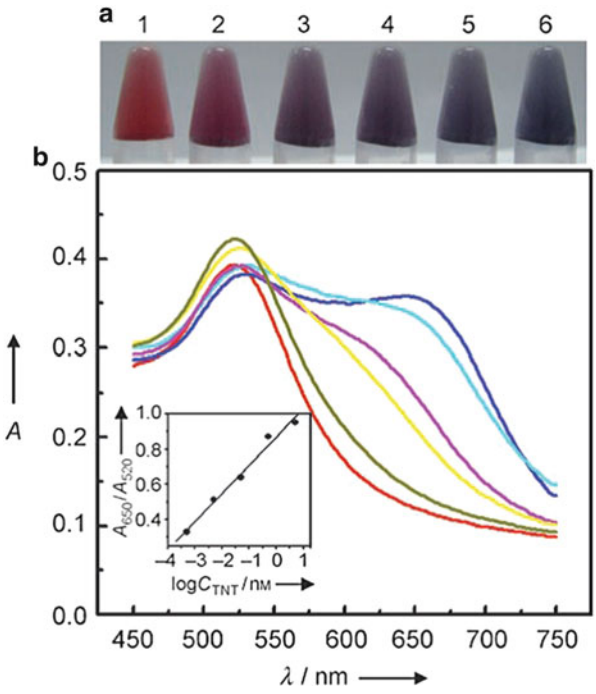

Fig. 8.2 (**a**) Colorimetric visualization of TNT by using Au NPs (containing 500 nM cysteamine). TNT concentrations varied from 5×10^{-13} (2) to 5×10^{-9} M (6). (**b**) UV/Vis spectra of the Au NPs suspension (10 nM) containing 500 nM cysteamine in the presence of different concentrations of TNT: *red*, 0 M; *dark yellow*, 5×10^{-13} M; *yellow*, 5×10^{-12} M; *magenta*, 5×10^{-11} M; *cyan*, 5×10^{-10} M; *blue*, 5×10^{-9} M. *Inset*: plot of A_{650}/A_{520} against log C_{TNT} for TNT assay [21]

and chemical sensors and this has been known for long time [11, 22]. Ying Jiang reported a simple and sensitive method for the colorimetric visualization of TNT at picomolar levels by using gold nanoparticles [21]. In this study, cysteamine was used both as the primary amine and as the stabilizer for Au NPs to facilitate the Donor–Acceptor interaction between TNT and the primary amine at the Au NP solution interface for direct visualization of TNT, based on the TNT-induced colorimetric nano-gold aggregation phenomenon.

Figure 8.2 demonstrated the colorimetric visualization of TNT by using Au NPs. Initially, the cysteamine-stabilized Au NPs were well dispersed in distilled water and the color of the uniform suspension was wine red, because of the strong surface plasmon resonance of the Au NPs. The addition of TNT to the dispersion essentially leads to the aggregation of the cysteamine-stabilized Au NPs as a result of the Donor-Acceptor (D–A) interaction between TNT and cysteamine, and the color of the suspension is accordingly changed to violet blue. The clear change in the color of the suspension could be used for the direct colorimetric visualization of TNT. As such a color change can be readily seen by the naked eye.

Zhang K et al. prepared ratiometric fluorescence probe comprising dual-emission QDs and the establishment of its utility for instant, on-site, and visual identification of TNT particulates deposited on various package surfaces such as manila envelopes, synthetic fabric bags, and rubber materials [24b]. They have prepared two different sized Cadmium telluride (CdTe) QDs emitting red and green

fluorescence's, respectively; have been hybridized by embedding the red-emitting one in silica nanoparticles and covalently linking the green-emitting one to the silica surface, respectively, to form a dual-emissive fluorescent hybrid nanoparticle. The fluorescence of red QDs in the silica nanoparticles stays constant, whereas the green QDs functionalized with polyamine can selectively bind TNT by the formation of Meisenheimer complex, leading to the green fluorescence quenching due to resonance energy transfer. The variations of the two fluorescence intensity ratios display continuous color changes from yellow-green to red upon exposure to different amounts of TNT.

The response of the dual-wavelength fluorescence intensity of the green emission from the reactive small QDs is gradually decreased by the addition of TNT, whereas the intensity of the red emission from the encapsulated large QDs still remains constant (Fig. 8.3a). The changes in the intensity ratio of the two emission wavelengths result in a continuous fluorescence color evolution (Fig. 8.3, bottom panel). Clearly, even a slight decrease of the green emission intensity leads to an obviously distinguishable color from the original background with the naked eye. The advantages of the ratiometric fluorescence for visual detection can be confirmed by the comparison with the single fluorescence quenching experiments which are employed in most of the current fluorometry for TNT detection (Fig. 8.3b). It can be seen that, unlike the ratiometric probe, the fluorescence images of the pure green QDs are hard to distinguish among the other images by the naked

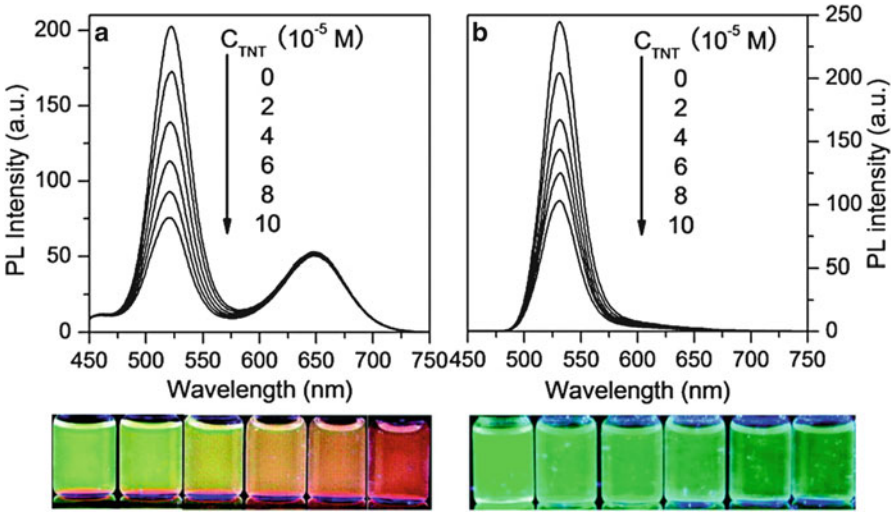

Fig. 8.3 Dependence of the fluorescence spectra ($\lambda_{ex} = 365$ nm) of (**a**) the ratiometric probe and (**b**) the *pure green* QDs modified with polyallylamine upon the exposure to different amount of TNT. (*Bottom panel*) Comparison between the fluorescence colors of the ratiometric probe solutions (*left*) and the *pure green* QDs solutions (*right*) after exposure to TNT. The concentrations of TNT from *left* to *right* are 0, 2×10^{-5}, 4×10^{-5}, 6×10^{-5}, 8×10^{-5}, and 10×10^{-5} mol/L, respectively. All the photos were taken under a 365 nm UV lamp [24b]

eye. The comparison clearly shows that the ratiometric fluorescence method is more sensitive and reliable for visual detection of TNT than a single fluorescence quenching method, although the intensity of the green emission decreases at the same level.

The collective oscillation of surface electrons on metal nanostructured materials has been leveraged for the amplification of optical processes in Raman scattering. The phenomenon of surface enhanced Raman scattering (SERS) is generally explained by a combination of an electromagnetic (EM) mechanism describing the surface electron movement in the substrate and a chemical mechanism related to charge transfer (CT) between the substrate and the analyte molecules. The possibility of observing raman signals, which are normally very weak, with enhancements of the order of and the unique ability to obtain molecular recognition of an analyte at very low concentrations in aqueous environment allow SERS to be unique for ultrasensitive biological and chemical analysis and environmental sensing. Based on unique SERS properties of cysteine modified gold nanoparticle, Samuel S. R. Dasary reported cysteine modified gold nanoparticle based miniaturized, inexpensive ultrasensitive SERS probe, for highly sensitive and selective screening of TNT from aqueous solution in 2 picomolar (pM) level [25]. Due to the formation of meisenheimer complex between TNT and cysteine, gold nanoparticles undergo aggregation in the presence of TNT via electrostatic interaction between meisenheimer complex bound gold nanoparticle and cysteine modified gold nanoparticle illustrated in Fig. 8.4. The reported SERS assay is rapid and takes less than 10 min from TNT binding to detection and analysis.

8.3 Smart Hybrid Sensor

The reported successful techniques being mostly solution-based have resulted in stability problems, limiting their potential ability and practical applications. Moreover, the response towards analyte predominantly monitored in situ, with respect to optical responses (color changes, intensity variation, shift in the emission spectra) making the sensor inefficient. This necessitates a need to develop a novel and modernistic method to fabricate a solid template-based sensor on a large scale for technological applications. A very few methods effectively demonstrated the sensing permanence of TNT in real time application [16, 26–36]. For example Daming Gao reported a resonance energy transfer-amplifying fluorescence quenching at the surface of silica nanoparticles for the ultrasensitive detection of TNT in solution and vapor environments [17]. They have modified the surface of silica nanoparticles with fluorescent dye and amine ligands. The formed hybrid can specifically bind TNT species by the charge-transfer complexing interaction between electron-rich amine ligands and electron-deficient aromatic rings.

The resultant TNT–amine complexes bound at the silica surface can strongly suppress the fluorescence emission of the chosen dye by the FRET from dye donor to the irradiative TNT–amine acceptor through intermolecular polar–polar

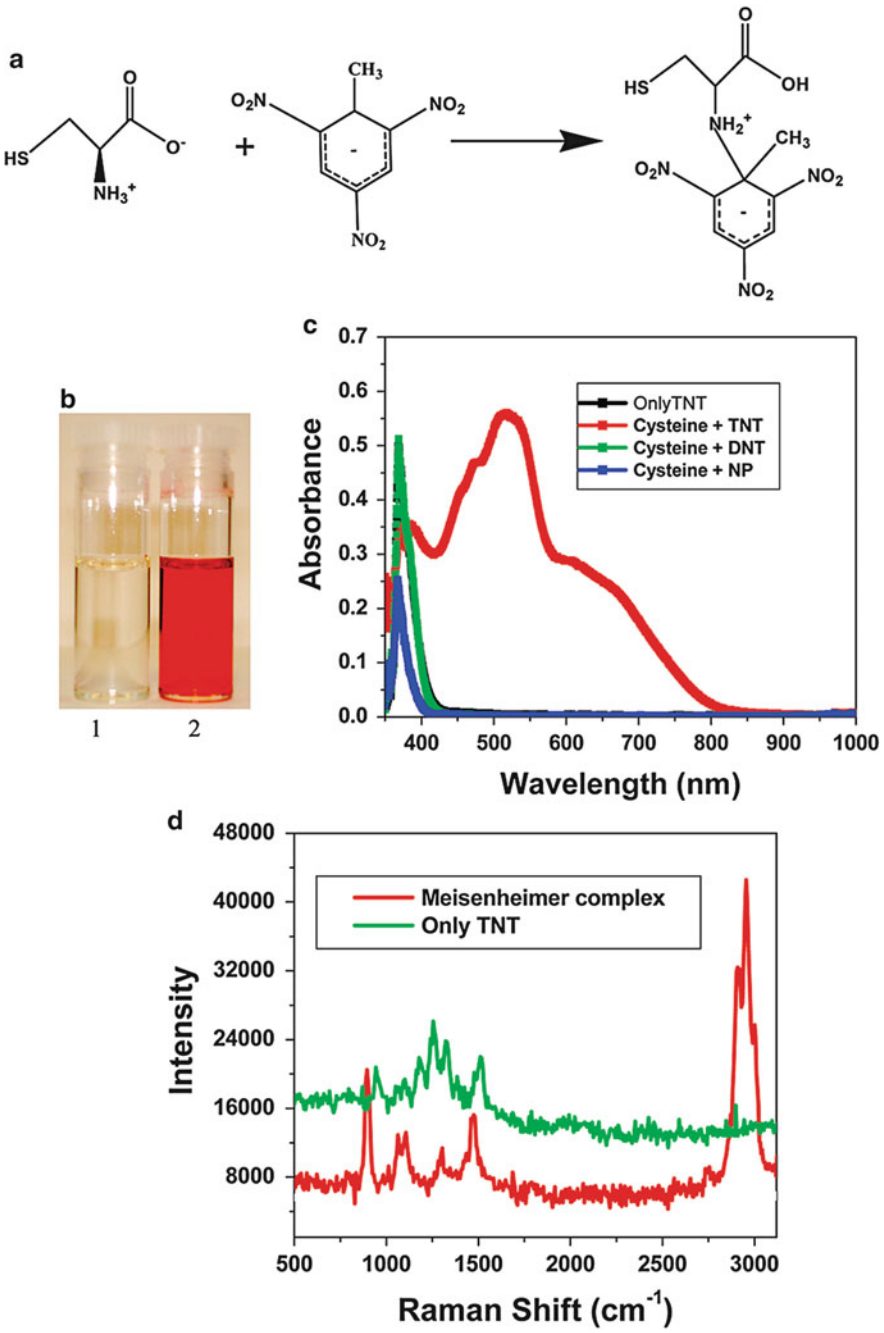

Fig. 8.4 (**a**) Schematic representation of the formation of Meisenheimer complex between cysteine and TNT, (**b**) Photograph showing how TNT changes the color when it forms Meisenheimer complex with cysteine (10 mM cysteine + 1 mM TNT), (1) 1 mM only TNT, (2) Meisenheimer complex after addition of 10 mM cysteine in 1 mM TNT. (**c**) absorption spectra demonstrating new peaks at 520 and 630 nm due to the formation of Meisenheimer complex in presence of 1 mM TNT. (**d**) Normal Raman spectra from 10 mM TNT and Meisenheimer complex

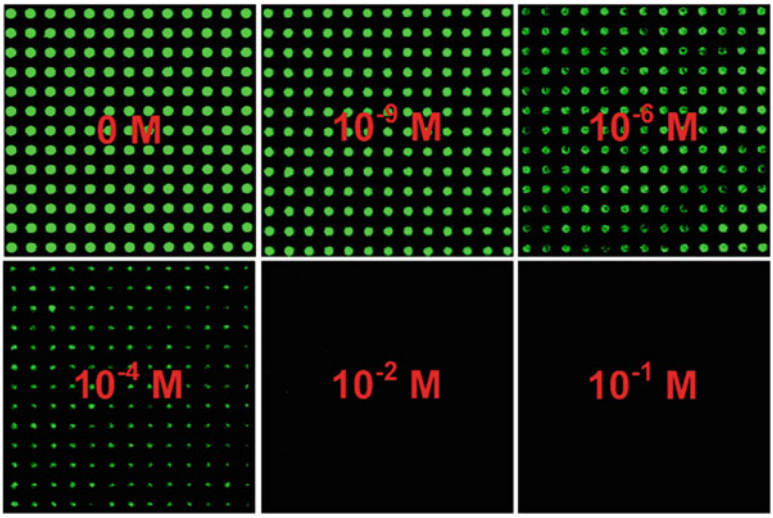

Fig. 8.5 Regular array assembly of fluorescein isothiocyanate (FITC) -NH_2-silica nanoparticles on the silicon wafer with etched microwells. Confocal fluorescence images show the evolution of the brightness and size of fluorescent dots on dropping 10 μL of TNT solution of different concentrations [17]

interactions at spatial proximity. Figure 8.5 shows the colorful fluorescence images under laser excitation on a confocal microscope. The fluorescent dot array is highly regular and extremely bright, and all microwells are completely filled with the fluorescent silica particles. The evolution of the brightness and size of fluorescent dots is clearly observed by dropping only 10 μL of TNT solution of different concentrations onto the 1×1 cm^2 sized chip. The brightness and size of fluorescent dots become smaller and smaller and ultimately disappear with the increase of concentration from 1×10^{-9} to 10^{-1} M. However, the nanoparticle chip seems to have a more sensitive response to the ultratrace amount of TNT than the nanoparticle suspensions. As shown in the Fig. 8.5, 10 μL of 1 nM TNT can result in a surprising reduction of the brightness and size of fluorescent dots under confocal microscope. It is thus estimated that 2 pg of TNT can clearly be detected using the nanoparticle-assembled chip. Moreover, one of the main advantages of the detection chips is that less amount of sample is needed for an ultratrace-level detection, due to the collective effect of particle assembly in the microwells. Therefore, the microchips can be used as a convenient indicator of TNT residues.

Kalathil K. Kartha reported that a fluorescent organogelator exhibits superior detection capability for TNT in the gel form when compared to that in the solution state [37]. The gel when coated on disposable paper strips detects TNT at a record attogram (ag, 10^{-18} g) level (12 ag/cm^2) with a detection limit of 0.23 ppq. The contact-mode response to TNT by the filter paper strips was tested by placing TNT

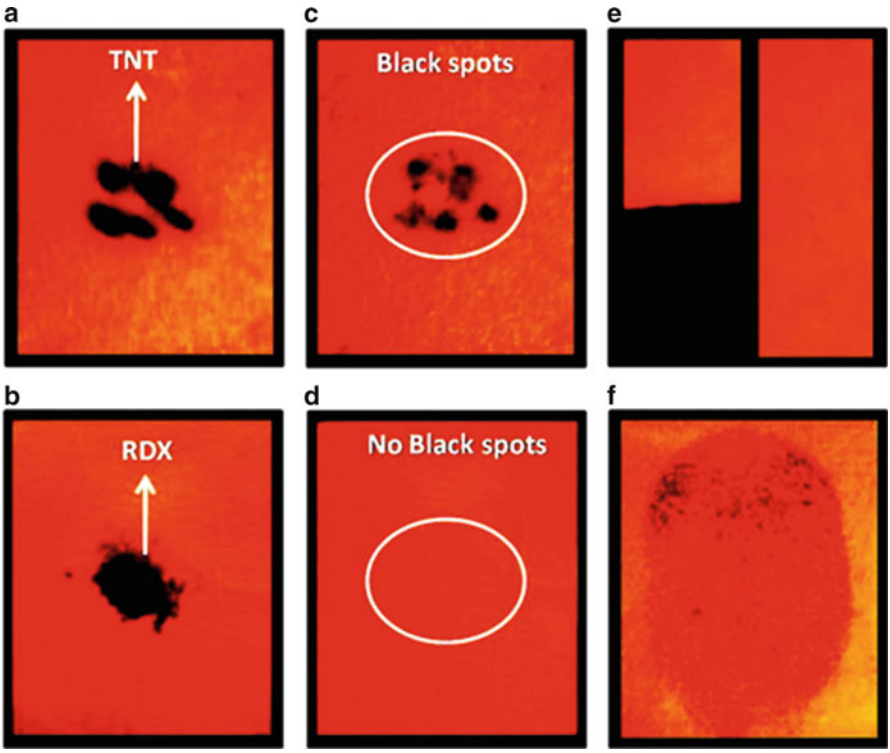

Fig. 8.6 Photographs of perfluoroarene-based gelator coated test strips under different experimental conditions. (**a**) TNT and (**b**) RDX crystals on *top*. (**c**, **d**) Corresponding photographs upon removal of the crystals after 5 s. (**e**) After dipping into solutions of TNT (*left*) and RDX (*right*) in acetonitrile (1×10^{-3} M). (**f**) Thumb impression after rubbing with TNT crystals (All photographs were taken under 365 nm UV illumination [37])

crystals over a test strip for 5 s, resulting in black spots upon illumination with a UV lamp (Fig. 8.6a, c). The same experiment was repeated with 1,3,5-trinitro-1,3,5-triazinane (RDX), and no spots corresponding to fluorescence quenching were found (Fig. 8.6b, d).

In addition, the test strips were dipped into acetonitrile solutions of TNT and RDX, and fluorescence quenching was observed only in the case of TNT (Fig. 8.6e). In another experiment, a human thumb was rubbed with TNT, and then all visible TNT particles were brushed off, followed by pressing the thumb against a test strip. The fingerprint of the thumb could be seen as quenched luminescence when illuminated with UV light (Fig. 8.6f). As a control experiment, the thumb (gloved) which was not contaminated with TNT was pressed on the test strip, and no fingerprint was seen. These images illustrate the utility of the gel-coated test strips for the on-site instant visualization of trace residues of TNT present on a specimen. Christina M. Gonzalez also reported the dodecyl groups

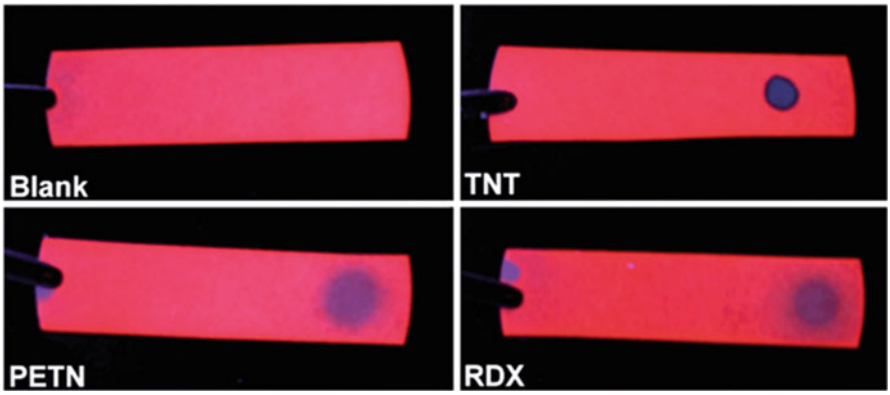

Fig. 8.7 Images of Si-NC coated filter paper under a handheld UV-lamp without the presence of nitrocompounds and in the presence of solutions of TNT, PETN, and RDX, as indicated [38]

functionalized luminescent silicon nanocrystals (Si-NCs) for nitroexplosive detection [38]. They found that Si-NC luminescence was quenched upon exposure to nitroaromatics via an electron transfer mechanism and a straightforward paper-based Si-NC sensor was developed which is found to be sensitive to solution, vapor, and solid phase nitroaromatics, as well as solution borne RDX and pentaerythritol tetranitrate (PETN) as illustrated in Fig. 8.7.

The meticulous animals changes their skin color to communicate, to express mood, for camouflage, or to respond to environmental changes due to their various nano and microscale components in their tissues [39–41]. Inspired by nature, sensors are being developed that change color in response to target chemicals by employing biomimetic structures and mechanisms. Jin-Woo Oh reported the self-assembly of genetically engineered viruses (M13 phage) into target-specific colorimetric biosensors [42]. The sensors are composed of phage-bundle nanostructures and exhibit viewing-angle independent color, similar to collagen structures in turkey skin.

On exposure to various volatile organic chemicals, the structures rapidly swell and undergo distinct color changes. Furthermore, sensors composed of phage displaying TNT binding peptide motifs identified from a phage display selectively distinguish TNT down to 300 ppb. As the concentration of applied TNT vapor increased, the TNT–Phage litmus showed pronounced color changes due to structural changes induced by TNT binding illustrated in Fig. 8.8. Moreover they confirmed that TNT binding to TNT–Phage litmus through Fourier transform–infrared spectroscopy analyses. They analyzed the specificity of the phage matrices, by comparing the sensing performance of DNT and MNT. On exposure to TNT (20 ppm), DNT (20 ppm) and MNT (300 ppm) vapor, the TNT–Phage litmus showed selective response to the TNT molecules, more than three and five times higher compared with DNT and MNT, respectively (Fig. 8.8c).

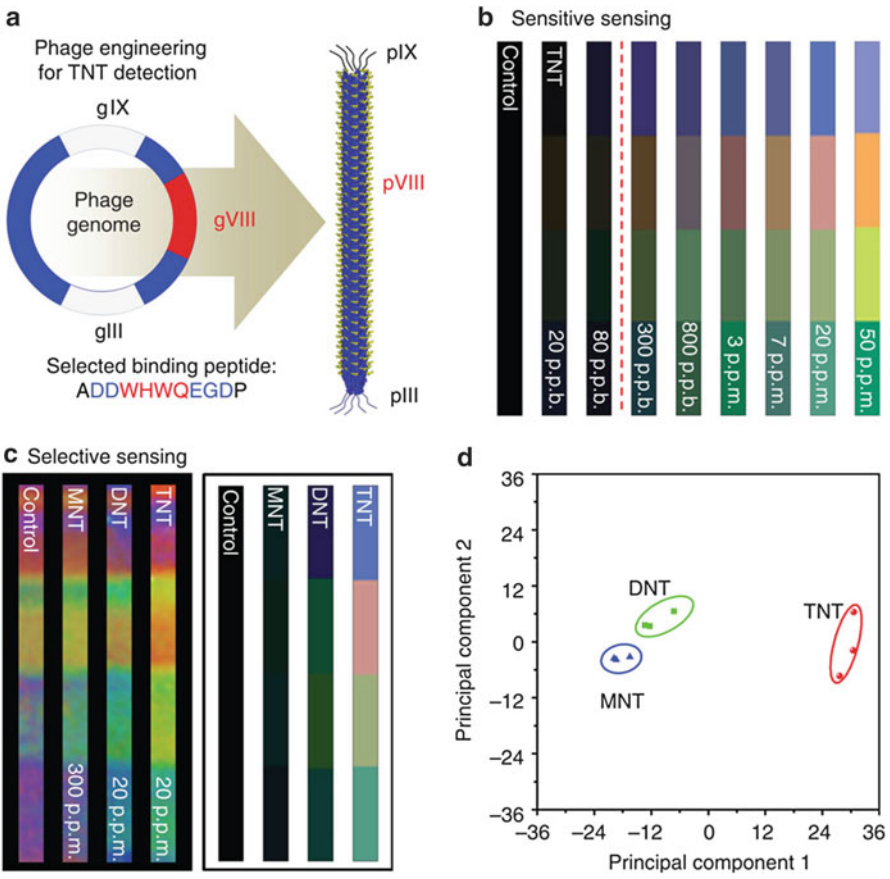

Fig. 8.8 (**a**) Two thousand and seven hundred copies of the TNT-binding receptor identified by directed evolution are genetically engineered onto the surface of M13 phage (TNT phage). (**b**) Using the iPhone-based analysis system, TNT is detectable down to 300 ppb in the gas phase. The *dashed redline* indicates the sensitivity limit of the TNT–Phage litmus against TNT. (**c**) Photos and processed color fingerprints from the TNT–Phage litmus after TNT, DNT and MNT exposure. The TNT–Phage litmus selectively detects the target TNT (20 ppm) over other molecules with similar chemical structures, such as DNT (20 ppm) and MNT (300 ppm). (**d**) Principal component analysis plot of the color changes resulting from the exposure of the Phage litmus to TNT, DNT and MNT [42]

8.3.1 *Fluorescent Electrospun Nanofibers for Explosive Detection*

Recently, much attention has been paid to the development of novel sensing materials for explosives in terms of improved sensitivity and selectivity [43]. However, it should be notable that multiple procedures are still required to fabricate such fascinating materials with controlled one dimensional structure. Compared with various chemical and physical methods have been developed so far, fluorescence-

based sensing performance attracts much consideration due to its high sensitivity and simplicity. However, the required multi-step processes restrict their practical applications in somewhat. To overcome this limitation, the researchers were adopted electrospinning technique to prepare one dimensional nanofiber and extended to incorporate various kinds of active materials in to them [44–51]. Yanke Che reported that nanoporous nanofibers fabricated from carbazole-based tetracycles allow for slow diffusion and strong encapsulation of TNT molecules within the nanopores, thus resulting in postexposure fluorescence quenching behavior, which enables selective detection of TNT among other common nitroaromatic explosives and oxidizing reagents [52].

Feng Wang demonstrates a new electrochemical method for the detection of ultratrace amount of TNT with synthetic copolypeptide-doped polyaniline nanofibers [53]. The copolypeptide, comprising of glutamic acid (Glu) and lysine (Lys) units, is in situ doped into polyaniline through the protonation of the imine nitrogen atoms of polyaniline by the free carboxylic groups of Glu segments, resulting in the formation of polyaniline nanofibers of emeraldine salt. The free amino groups of Lys segments at the surface of nanofibers provide the receptor sites of TNT through the formation of charge–transfer complex between the electron-rich amino groups and the electron-deficient aromatic rings.

The schematic representation of the structure of poly(Glu-Lys)-doped Polyaniline (PANI) nanofibers and their specific interaction with TNT molecules is illustrated in Fig. 8.9. Adsorptive stripping voltammetry results demonstrate that

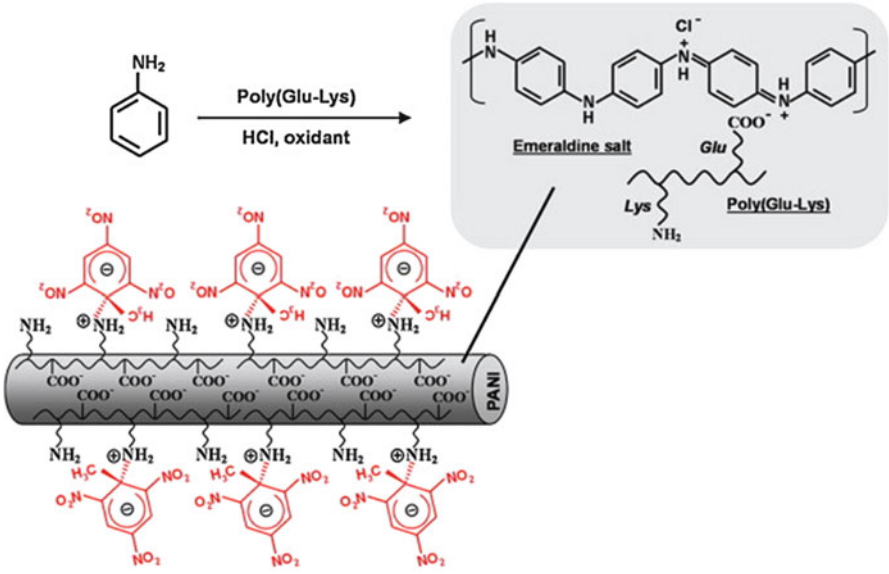

Fig. 8.9 Schematic illustrations for synthesis and structure of poly(Glu-Lys)-doped PANI nanofibers. The *bottom-left inset* shows the specific interaction between the doped nanofiber and TNT molecules through the formation of charge–transfer complex [53]

the poly(Glu-Lys)-doped nanofibers confined onto glassy carbon electrodes exhibit a remarkable enriching effect and thus sensitive electrochemical response to TNT with a linear dynamic range of 0.5–10 μM and a detection limit down to 100 nM.

It is well known that solid state sensing material for highly desired for vapor detection. In most cases, the performance is readily depends on the film thickness, which might be due to the slow diffusion of analyte vapors into the films. To reduce the dependence of sensing performance on film thickness, a highly porous nanostructure could be a solution, mainly attributed to their large surface to volume ratio, inherently high porosity, and easy accessibility of sensing materials. In this regard, electrospinning has emerged in recent years as a simple and cost-effective approach to fabricate nonwoven nanofibrous polymer composite films with high porosity and flexibility, which has great potential for enhanced explosives detection.

Ying Wang developed the electrospun fluorescent nanofibrous membrane of pyrene/polystyrene/tetrabutylammonium hexafluorophosphate (pyrene/PS/TBAH) via electrospinning for the detection of ultra-trace nitro explosive vapors and buried explosives by naked eye under UV excitation [54]. The schematic illustration of experimental setup for evolution of electrospun pyrene/PS/TBAH films towards nitro-explosive vapors is presented in Fig. 8.10. Under UV light, the fluorescence quenching upon the exposure of the as-electrospun film to various sub-equilibrium vapors could be observed by naked eye (Fig. 8.10c). The dark spots on the luminescent sensing films indicate the quenching of the as-electrospun pyrene/PS/TBAH by analyte vapors. Clearly, all nitramine and nitrate ester explosives could be discriminated by their sub-equilibrium vapors generated from nanogram residues. The sub-equilibrium vapors from 10 ng of RDX and PETN could produce acceptable dark quenching circles and visualized by naked eye after 20 min, and down to 1 ng of RDX and PETN could be visualized with an extended exposure time of 2 h. The time for octahydro-1,3,5,7-tetranitro-1,3,5,7-tetrazocine (HMX) detection took considerably longer time (2 h for 1 μg, and 12 h for 1 ng) due to its extremely low volatility.

The performance of the developed sensor is very impressive, considering the fact that the tested vapors were generated from freshly spotted explosive residues in an open environment with concentrations much lower than their equilibrium or saturated vapor concentration (e.g. 0.1 ppt for HMX, 5 ppt for RDX, 7 ppt for PETN, and 74 ppt for Tetryl) and the detection was conducted without the use of any piece of advanced instruments. The observed dramatic quenching in its fluorescence emission is due to the high binding affinity between the electron-deficient nitro explosives and the sensing film.

To clean up the unexploded landmines, direct detection of buried explosives has emerged as a promising need. In this regard, they extended the application of as-electrospun pyrene/PS/TBAH nanofibrous membrane for buried explosives (2,4-DNT). Figure 8.11a–d shows the detection of explosives buried in soil using electrospun pyrene/PS/TBAH nanofibrous film coated filter paper. Due to the leaked explosive molecules from buried explosives, a strong fluorescence quenching can be observed in 10 min by naked eye under UV light.

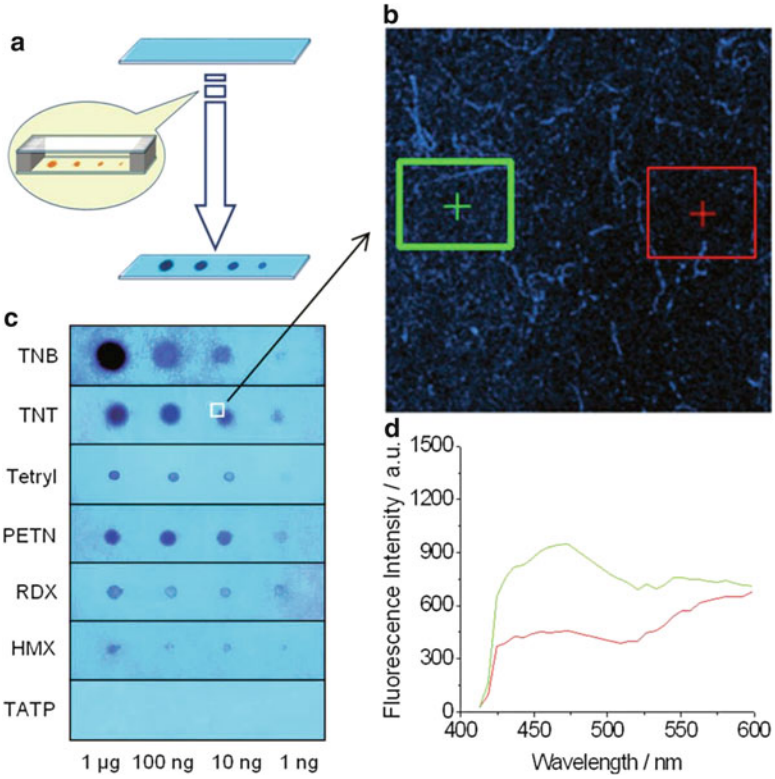

Fig. 8.10 (**a**) Schematic illustration of experimental setup for electrospun pyrene/PS/TBAH films towards sub-equilibrium nitro-explosive vapors; (**b**) the fluorescence microscopy image (λ ex 343 nm, λ em 470 nm) at the edge of the quenching spot in (**c**); (**c**) UV excited (λ ex 275 nm) images of 3- μ m thick films after exposure to sub-equilibrium vapors generated from 1 μ g, 100 ng, 10 ng, and 1 ng solid analytes; (**d**) emission profile (λ ex 343 nm) of the square area outside (*green*) and inside (*red*) the quenching spot in (**b**) [54]

The quenching spots indicated the position of buried explosives, while other parts without explosives are still glowing. It is worth noting that the electrospun sensing film on filter paper does not directly contact with soil samples. Therefore, the quencher is solely the leaked 2,4-DNT vapor that penetrates through the soil and filter paper. In recent past, Metal-organic frameworks (MOFs) have been gained enormous attention due to their distinct features including high porosity, large surface area, and flexible skeleton [55, 56]. Moreover, considerable attention also paid to produce MOF membranes by growing continuous MOF crystals on porous substrates. Thereby, the development of chemical sensors based on MOFs has drawn considerable attention due to their flexible structures responsive to external stimulation. Yunxia Xu reported the example of using electrospun nanofibrous mats as skeletons to produce MOF membranes, and demonstrated the great potentials of

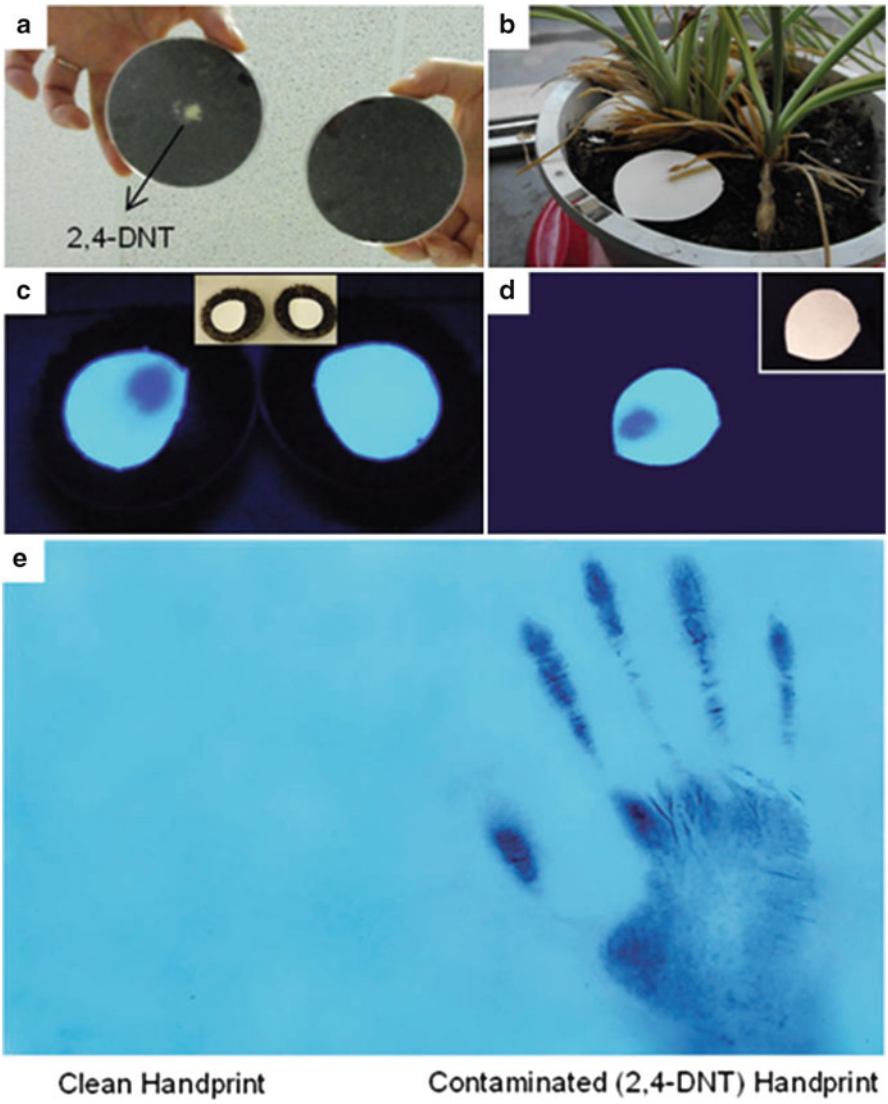

Fig. 8.11 (**a**–**d**) Above-ground detection of buried 2,4-DNT using the electrospun pyrene/PS/TBAH films (3- μ m thick, figures are taken at 30 min exposure time for a better visibility): (**a**) Optical images of soil with (*left*) and without (*right*) buried 2,4-DNT in Petri dishes; (**b**) optical images of soil with buried DNT in a flower pot; (**c**) UV (λ ex 275 nm) excited image of electrospun sensing films on buried DNT in a Petri dish after 30 min exposure time; (**d**) UV (λ_{ex} 275 nm) excited image obtained from the test of electrospun sensing film on 2,4-DNT buried in a flower pot after 30 min. Insets in (**c**) and (**d**) are the bright-field images of same membranes after detection; (**e**) detection of particulate explosives contaminated hand using the electrospun pyrene/PS/TBAH films [54]

such nonwoven fiber mats as a new kind of porous supports in MOF research field [57]. Macroporous network structure of Zn-MOF/PST-1 thin films prepared by using electrospinning technique.

The secondary growth technique was further developed to strongly anchor Zn-MOF seed crystals on porous supports Zn-MOF/PST-1 to form Zn-MOF/PST-2 thin films. Figure 8.12 illustrates characterization of Zn-MOF/PST-1 and Zn-MOF/PST-2. Following this, they were performed the fluorescence quenching experiments to demonstrate the ability of Zn-MOF/PST-2 thin films for detection of

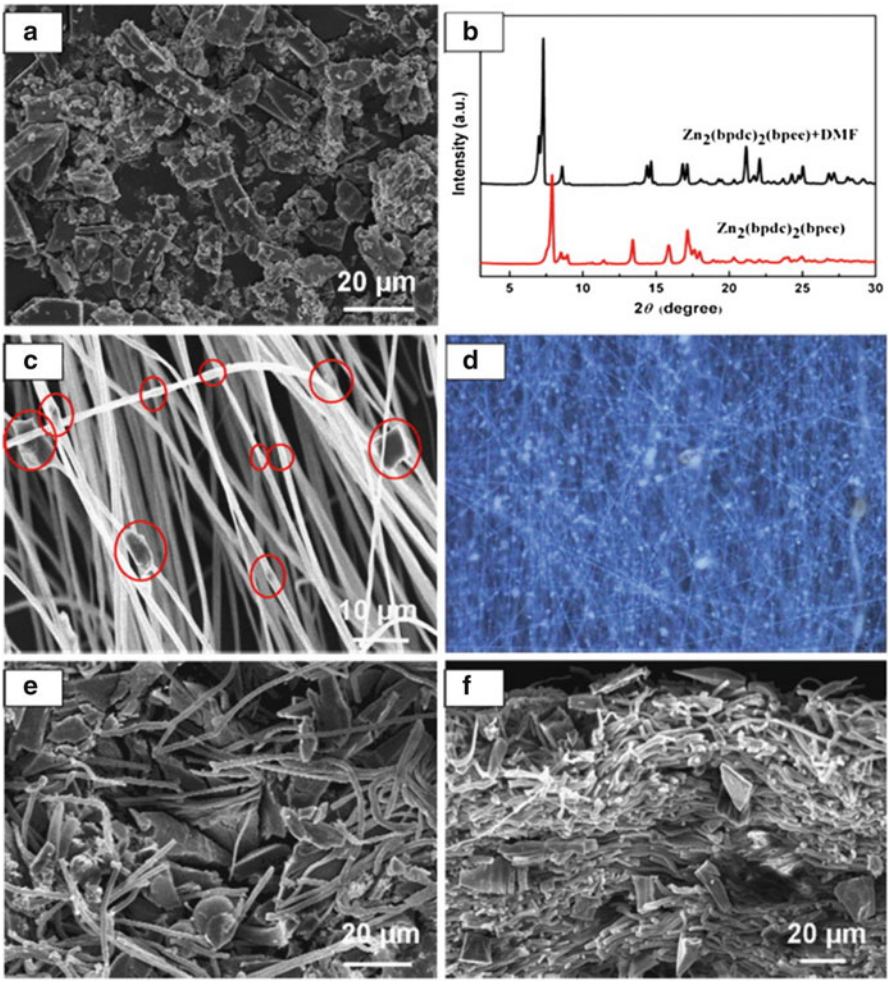

Fig. 8.12 (**a**) SEM image and (**b**) XRD pattern of the [Zn_2(bpdc)2(bpee)] crystals; (**c**) SEM image and (**d**) fluorescent image of Zn-MOF/PST-1 thin film; (**e**) *top* view and (**f**) cross-sectional SEM image of Zn-MOF/PST-2 thin film by secondary growth [57]

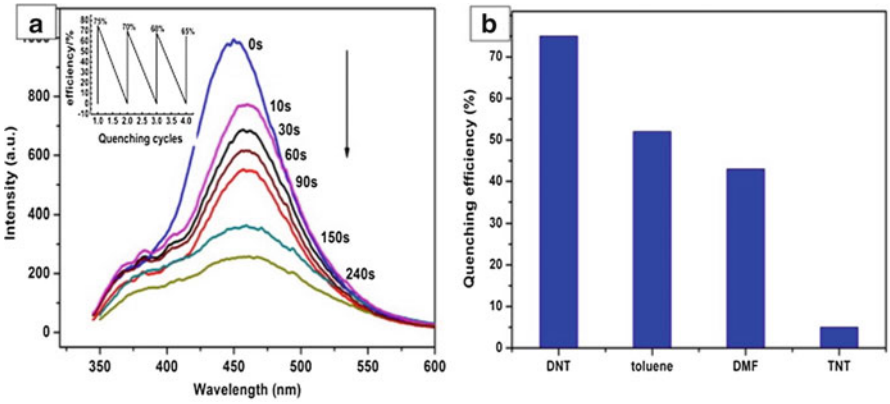

Fig. 8.13 (**a**) Fluorescence quenching of Zn-MOF/PST-2 films upon exposure to DNT vapor from 0 to 240 s, and (**b**) the percentage of fluorescence quenching of Zn-MOF/PST-2 films with four different vapors: DNT, toluene, DMF, TNT [57]

nitroaromatic explosives. Fluorescence response to vapors of DNT and TNT was certained by inserting the prepared films into glass vials (10 mL) which containing 1.5 g solids DNT and TNT powder and cotton gauze. Figure 8.13a shows the fluorescence intensity evolution of Zn-MOF/PST-1 film upon exposure to saturated DNT vapor for 60 s. About 5 % fluorescence quenching happened in the first 10 s, and finally 24 % quenched after 60 s. According to fluorescence quenching data shown in Fig. 8.13b, the quenching intensity of Zn-MOF/PST-2 film was increased to 42 % after exposure for 60 s. The higher quenching efficiency attributes to more particles on the surface and inside of Zn-MOF/PST-2 film, compared with particles only inside of the Zn-MOF/PST-1 film.

Yang et al. developed a tetrakis(4-methoxylphenyl)porphyrin (TMOPP) and polystyrene based electrospun nanofibrous film sensor for detection four nitroaromatic explosives [58]. Porphyrins as an obvious class of electron-donating dyes are very attractive for sensing devices. The sensing of explosive vapors were performed by keeping the 3 mg/3 μL of explosives at saturation vapor pressure in a 1 cm quartz cell with the fabricated sensing film.

Time-dependent fluorescence quenching was measured over 2 h of exposure towards the saturated explosive vapors in air. At room temperature the vapor pressures of DNT, TNT and picric acid (PA) are 280 ppb, 4 ppb, and 0.0077 ppb, respectively. After 40 min, the percentage of fluorescence quenching was 38 %, 17 %, 4 %, and 2 % for DNT, DNP, TNT and PA vapors, respectively. Because the vapor pressure of DNT is about 70-fold and 4×10^4 fold that of TNT and PA, respectively, the quenching percentage with TNT or PA vapor is thus surprisingly larger than that expected from the relative vapor pressure of these explosives. That means TMOPP-based electrospun nanofibrous films have the potential to

sensitively detect down to several parts-per-billion of TNT vapor or several parts-per-trillion of PA vapor in the atmosphere. The ultra sensitive detection of TNT is demonstrated by using porphyrinated polyimide nanofibers by Lv YY [59]. The covalent bonding of porphyrin fluorophores with polyimide main chains reduces the aggregation-caused fluorescence self-quenching of porphyrin and improved the physicochemical stability of the polyimide nanofibers.

Besides TNT, 2,4-dinitrotoluene (DNT), 2,4,6-trinitrophenol (PA) and nitrobenzene (NB) could also quench the fluorescence of the porphyrinated nanofibers, but the quenching efficiency is much lower than that of TNT. The time-dependent fluorescence quenching efficiency of the porphyrinated nanofibers exposed to different analytes is presented in Fig. 8.14. For those explosive vapors, TNT, DNT, NB and PA, the quenching efficiencies are in the order of TNT > DNT > NB > PA. Conjugated polymers (CP) have been recognized as one of the high-performance sensing probes due to their excellent molar absorptivity and fluorescence quantum. The fluorescence self-quenching behavior by self aggregation nature of CPs is a major disadvantage counteracting their application in chemical sensors.

Therefore, the combination of electrospinning with fluorescent CPs offers the potential application as a new and universal fabrication approach for chemosensory devices. Long Y et al. prepared electrospun nanofibrous film doped with a fluorescent conjugated polymer P as a sensory device for detection of the explosive

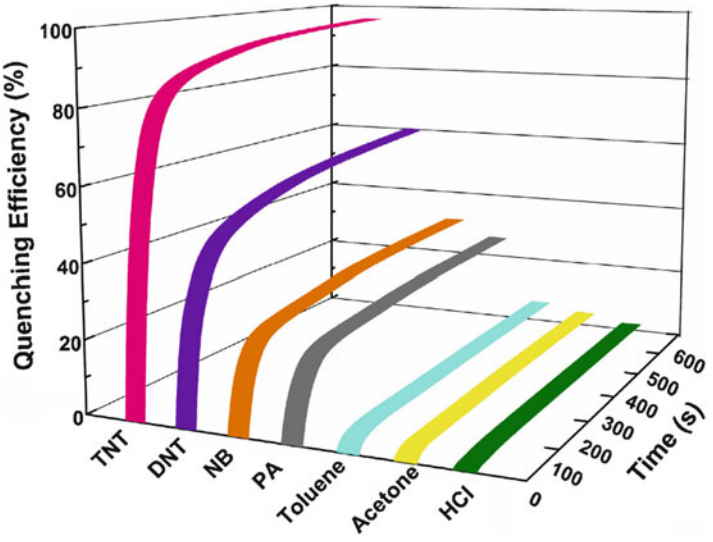

Fig. 8.14 Time-dependent fluorescence quenching efficiency of the porphyrinated nanofibers for different analytes (saturated vapors, except 30 ppm for HCl) [59]

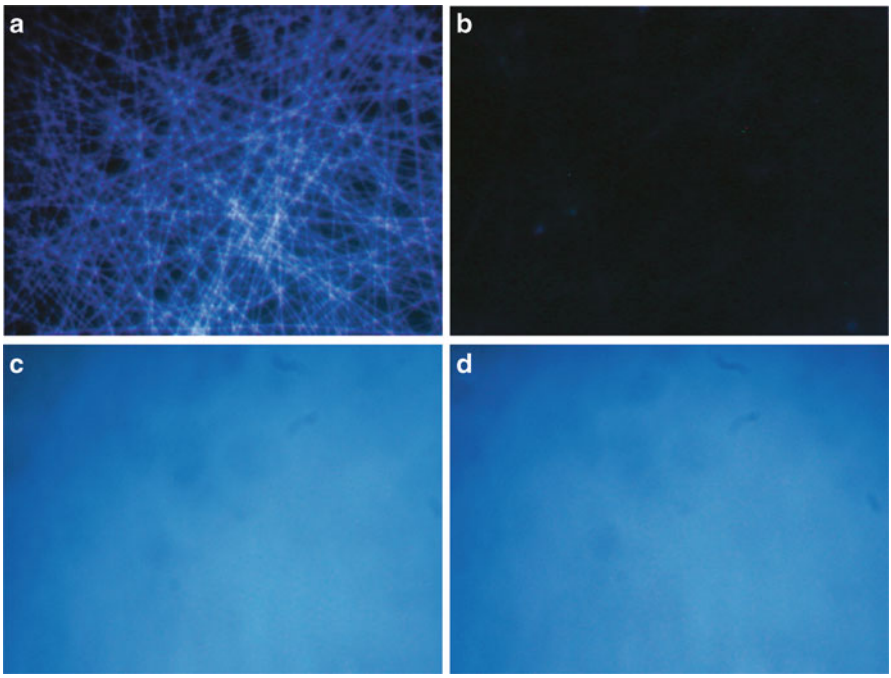

Fig. 8.15 Fluorescence images of electrospun nanofibers with porogen (**a**) before and (**b**) after being exposed to DNT vapor for 30 min and dense spin casting film (**c**) before and (**d**) after being exposed to DNT vapor for 30 min [60]

2,4-dinitrotoluene (DNT) [60]. Polymer P obtained through a sonogashira cross-coupling polymerization. The electrospinning technique effectively reduced aggregation and fluorescence self-quenching of the conjugated polymers. The efficient quenching towards DNT was clearly observed by visible using fluorescence microscopy (Fig. 8.15). In a control experiment, the fluorescence images of spin-casting film before and after the DNT exposure were taken and shown in Fig. 8.15. There was hardly any difference observed from this densely packed sensing film. And also Liao et al. prepared the blue light-emitting oligotriphenylene nanofibers by oxidizing triphenylene using ferric chloride, as fluorescent sensors for detecting traces of nitro-based explosives including nitromethane, nitrobenzene, and 2,4,6-trinitrophenol [61]. Shengyang Tao adopted a simple sol–gel chemistry and the electrospinning technique for the production of nanocomposite fibers [62]. Bridged organosilane was used as a cross-linker to form a viscous gel solution, and without the addition or help of polymer, generally used in the literature, nanocomposite fibers were conveniently fabricated at room temperature and were demonstrated as

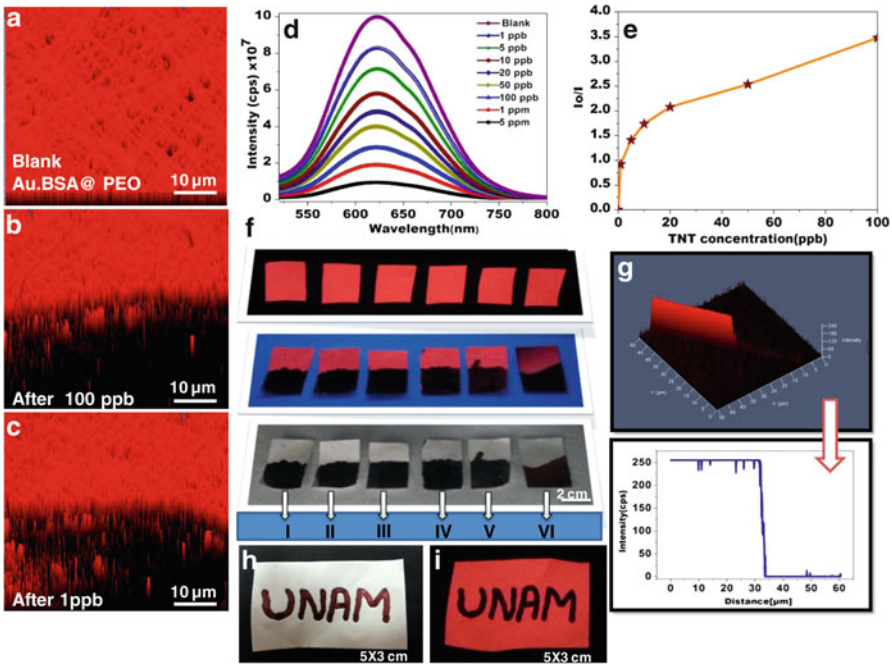

Fig. 8.16 (**a–c**) CLSM images of the Au.BSA@PEO-NFM on glass slides before (**a**) and after (**b–c**) exposure to TNT ($\lambda ext = 488$ nm, 20× magnification) (**d**) Fluorescence spectra of Au.BSA@PEO-NFM upon treatment of various concentration of TNT (**e**) The relative fluorescence intensity (I_0/I, where I and I_0 are the fluorescence intensity in the presence and absence of TNT, respectively) versus the TNT concentration (**f**) Photograph of the fluorescence quenching of Au.BSA@PEO-NFM strips by different concentration of TNT on contact mode when viewed under UV and white light (*I*-1 ppm, *II*-100 ppb, *III*-50 ppb, *IV*-20 ppb, *V*-10 ppb, *VI*-1 ppb). (**g**) TNT treated Au.BSA@PEO-SNF and their fluorescence intensity profile. (**h–i**) Au.BSA@PEO-NFM based TNT sensor for visual detection by hand writing on the Au.BSA@PEO-NFM using TNT solution as ink [63]

novel fluorescence-based chemosensors for the rapid detection of trace vapor (10 ppb) of explosive.

Anitha et al. demonstrated selective, on-the-spot detection of TNT at sub ppt level using a single nanofiber embedded fluorescent gold clusters hybrid system [63]. They have incorporated red fluorescent BSA-capped gold clusters into the PEO nanofibers termed as Au.BSA@PEO-NFM using a simple and straightforward electrospinning method. The use of polymeric matrix and the adopted method has allowed to attain a uniform dispersion of gold clusters in the nanofibers while at the same time maintaining its morphology. The sensing performance of Au.BSA@PEO NFM has been tested upon exposure to different concentration of TNT is presented in Fig. 8.16. The fluorescence intensity is clearly decreased as a function of increasing concentration of TNT which is demonstrated by CLSM images

(Fig. 8.16a–c). The fluorescence spectral changes of the Au.BSA@PEO-NFM for a wide range of TNT concentration has been picturised in Fig. 8.16d.

The relative fluorescence intensity (I_0/I, where I and I_0 are the fluorescence intensity in the presence and absence of TNT, respectively) versus the TNT concentration has been presented in Fig. 8.16e.

The visual fluorescence responses of Au.BSA@PEO-NFM at different concentrations of TNT by contact mode method have been tested by placing the nanofibrous membrane in the TNT solution for a second has been displayed in Fig. 8.16f. Immediately, the color of the Au.BSA@PEO-NFM changed from white to either deep red or blue depending on the concentration and time in normal light condition which clearly illustrates their utility for the onsite instant visualization of TNT. The ocular noticeable response of the hybrid nanofibrous membrane towards the TNT solution has been found to be at one parts per billion (1 ppb). Further, the known factor in sensing performance in their bulk state has been known to be limited by their cross linked nature. Moreover, the complete decrease in the fluorescence intensity at 1 ppb level of TNT in bulk state further projected to investigate their sensing performance on even lower concentrations using single nanofiber (SNF), due to which it will further reduce the outlay of the devices. As predicted, a SNF could sensitively detect the TNT molecules and showed enhanced detection limit of TNT that reaches a level up to sub ppt (0.1 ppt). The gradual decrease in the intensity, upon increasing the concentration is clearly observed at SNF level as presented in Fig. 8.17. The decrease in the luminescence intensity occurred consistently throughout the SNF and such admirable characteristics of uniformity are significant in the development of a trustworthy method. Fluorescent organic polymers also successfully made into the nanofibers and further used as a sensory probe for TNT detection [64–66].

8.4 Conclusions

In this chapter, we summarized initially the major advancement in the field of fluorescent nanohybrids from challenging synthesis to the promise application in TNT sensor. Despite substantial progress have been made, a diversity of challenges remains restricts their sensing performance in outdoor application. On the basis of the outlined achievements over the past few years, the electrospun nanofibers have been successfully adopted as a support for fluorescent probes and in some cases as a probe for improved sensitivity. The growing number of electrospun hybrid nanofiber systems might open a new venture in addressing important issues for detection of TNT in environmental application and we believe that the creation of new hybrid nanofiber for improved sensing performance will persistently grow over coming years.

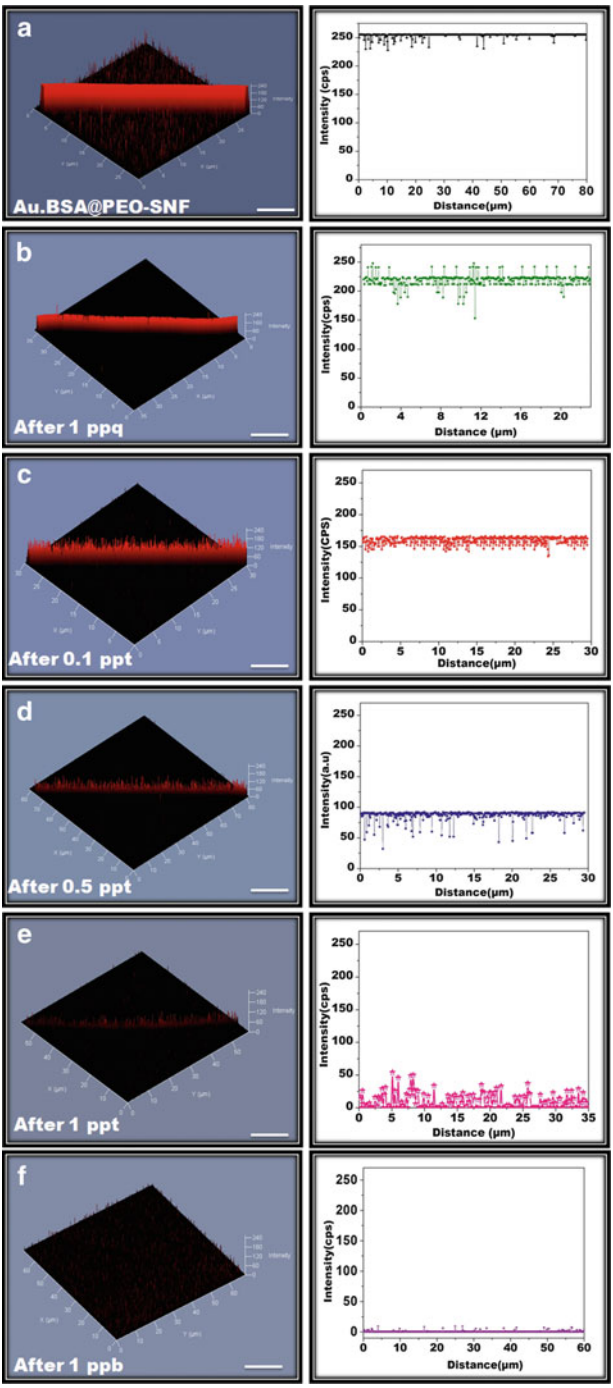

Fig. 8.17 CLSM images of Au.BSA@PEO-SNF upon exposure to different concentration of TNT and their intensity profile collected from the surface of the nanofiber (*scale bar* 10 μm) [63]

Acknowledgements Anitha Senthamizhan thanks the Scientific & Technological Research Council of Turkey (TUBITAK) (TUBITAK-BIDEB 2216, Research Fellowship Programme for Foreign Citizens) for postdoctoral fellowship. Tamer Uyar acknowledges partial support of EU FP7- Marie Curie-IRG for funding NANOWEB (PIRG06-GA-2009-256428) and The Turkish Academy of Sciences – Outstanding Young Scientists Award Program (TUBA-GEBIP).

References

1. R. Freeman, T. Finder, L. Bahshi, R. Gill, I. Willner, Functionalized CdSe/ZnS QDs for the detection of nitroaromatic or RDX explosives. Adv. Mater. **24**, 6416–6421 (2012)
2. Z.C. Symons, N.C. Bruce, Bacterial pathways for degradation of nitroaromatics. Nat. Prod. Rep. **23**, 845–850 (2006)
3. M. Kulkarni, A. Chaudhari, Microbial remediation of nitro-aromatic compounds: an overview. J. Environ. Manag. **85**, 496–512 (2007)
4. M.E. Honeycutt, A.S. Jarvis, V.A. McFarland, Cytotoxicity and mutagenicity of 2,4,6-TNT and its metabolites. Ecotoxicol. Environ. Saf. **35**(3), 282–287 (1996)
5. R. Martel, M. Mailloux, U. Gabriel et al., Behavior of energetic materials in ground water at an anti-tank range. J. Environ. Qual. **38**, 75–92 (2009)
6. J.D. Rodgers, N.J. Bunce, Treatment methods for the remediation of nitroaromatic explosives. Wat. Res. **35**(9), 2101–2111 (2001)
7. K. Ayoub, E.D. van Hullebusch, M. Cassir et al., Application of advanced oxidation processes for TNT removal: a review. J. Hazard. Mater. **178**, 10–28 (2010)
8. S.J. Toal, W.C. Trogler, Polymer sensors for nitroaromatic explosives detection. J. Mater. Chem. **16**, 2871–2883 (2006)
9. M.B. Pushkarsky, I.G. Dunayevskiy, M. Prasanna et al., High-sensitivity detection of TNT. PNAS **103**(52), 19630–19634 (2006)
10. L.A. Pinnaduwage, A. Gehl, D.L. Hedden et al., A microsensor for trinitrotoluene vapour. Nature **425**, 474 (2003)
11. M. Riskin, R. Tel-Vered, O. Lioubashevski et al., Ultrasensitive surface plasmon resonance detection of trinitrotoluene by a bis-aniline-cross-linked Au nanoparticles composite. J. Am. Chem. Soc. **131**, 7368–7378 (2009)
12. S. Kumar, N. Venkatramaiah, S. Patil, Fluoranthene based derivatives for detection of trace explosive nitroaromatics. J. Phys. Chem. C **117**, 7236–7245 (2013)
13. R. Tu, B. Liu, Z. Wang et al., Amine-capped ZnS-Mn^{2+} nanocrystals for fluorescence detection of trace TNT explosive. Anal. Chem. **80**, 3458–3465 (2008)
14. S.W.I.I.I. Thomas, G.D. Joly, T.M. Swager, Chemical sensors based on amplifying fluorescent conjugated polymers. Chem. Rev. **107**(4), 1339–1386 (2007)
15. G.H. Shi, Z.B. Shang, Y. Wang et al., Fluorescence quenching of CdSe quantum dots by nitroaromatic explosives and their relative compounds. Spectrochim. Acta Mol. Biomol. Spectrosc. **70**(2), 247–252 (2008)
16. J.S. Yang, T.M. Swager, Fluorescent porous polymer films as TNT chemosensors: electronic and structural effects. J. Am. Chem. Soc. **120**, 11864–11873 (1998)
17. D. Gao, Z. Wang, B. Liu et al., Resonance energy transfer-amplifying fluorescence quenching at the surface of silica nanoparticles toward ultrasensitive detection of TNT. Anal. Chem. **80**, 8545–8553 (2008)
18. Y. Engel, R. Elnathan, A. Pevzner et al., Supersensitive detection of explosives by silicon nanowire arrays. Angew. Chem. Int. Ed. **49**, 6830–6835 (2010)
19. G.B. Demirel, B. Daglara, M. Bayindir, Extremely fast and highly selective detection of nitroaromatic explosive vapours using fluorescent polymer thin films. Chem. Commun. **49**, 6140–6142 (2013)

20. Y. Chen, Z. Chen, Y. He et al., L-Cysteine-capped CdTe QS-based sensor for simple and selective detection of trinitrotoluene. Nanotechnology **21**, 125502 (2010)
21. Y. Jiang, H. Zhao, N. Zhu et al., A simple assay for direct colorimetric visualization of trinitrotoluene at picomolar levels using gold nanoparticles. Angew. Chem. Int. Ed. **47**, 8601–8604 (2008)
22. E.R. Goldman, I.L. Medintz, J.L. Whitley et al., A hybrid quantum dot-antibody fragment fluorescence resonance energy transfer-based TNT sensor. J. Am. Chem. Soc. **127**, 6744–6751 (2005)
23. M. Alcaniz, J.L. Vivancos, R. Masot et al., Design of an electronic system and its application to electronic tongues using variable amplitude pulse voltammetry and impedance spectroscopy. J. Food Eng. **111**, 122–128 (2012)
24. (a) Yunsheng Xia, Lei Song, and Changqing Zhu, Turn-on and near-infrared fluorescent sensing for 2,4,6-trinitrotoluene based on hybrid (gold nanorod)−(quantum dots) Assembly. Anal. Chem. **83**(4), 1401–1407 (2011); (b) K. Zhang, H. Zhou, Q. Mei et al., Instant visual detection of trinitrotoluene particulates on various surfaces by ratiometric fluorescence of dual-emission quantum dots hybrid. J. Am. Chem. Soc. **133**(22), 8424–8427 (2011)
25. S.S.R. Dasary, A.K. Singh, D. Senapati et al., Gold nanoparticle based label-free SERS probe for ultrasensitive and selective detection of trinitrotoluene. J. Am. Chem. Soc. **131**, 13806–13812 (2009)
26. Q. Fang, J. Geng, B. Liu et al., Inverted opal fluorescent film chemosensor for the detection of explosive nitroaromatic vapors through fluorescence resonance energy transfer. Chem. Eur. J. **15**, 11507–11514 (2009)
27. H. Sohn, R.M. Calhoun, M.J. Sailor et al., Detection of TNT and picric acid on surfaces and in seawater by using photoluminescent polysiloles. Angew. Chem. **40**(11), 2104–2105 (2001)
28. P.C. Chen, S. Sukcharoenchoke, K. Ryu et al., 2,4,6-Trinitrotoluene (TNT) chemical sensing based on aligned single-walled carbon nanotubes and ZnO nanowires. Adv. Mater. **22**, 1900–1904 (2010)
29. A.D. Aguilar, E.S. Forzani, M. Leright et al., A hybrid nanosensor for TNT vapor detection. Nano Lett. **10**, 380–384 (2010)
30. A. Rose, Z. Zhu, C.F. Madigan et al., Sensitivity gains in chemosensing by lasing action in organic polymers. Nature **434**, 876–879 (2005)
31. A. Lan, K. Li, H. Wu et al., A luminescent microporous metal–organic framework for the fast and reversible detection of high explosives. Angew. Chem. Int. Ed. **48**, 2334–2338 (2009)
32. K. Cizek, C. Prior, C. Thammakhet et al., Integrated explosive preconcentrator and electrochemical detection system for 2,4,6-trinitrotoluene (TNT) vapor. Anal. Chim. Acta. **661**, 117–121 (2010)
33. C.X. Guo, Z.S. Lu, Y. Lei et al., Ionic liquid–graphene composite for ultratrace explosive trinitrotoluene detection. Electrochem. Commun. **12**, 1237–1240 (2010)
34. H.X. Zhang, A.M. Cao, J.S. Hu et al., Electrochemical sensor for detecting ultratrace nitroaromatic compounds using mesoporous SiO_2-modified electrode. Anal. Chem. **78**, 1967–1971 (2006)
35. M. Riskin, R. Tel-Vered, T. Bourenko et al., Imprinting of molecular recognition sites through electropolymerization of functionalized Au nanoparticles: development of an electrochemical TNT sensor based on π-donor-acceptor interactions. J. Am. Chem. Soc. **130**, 9726–9733 (2008)
36. S. Hrapovic, E. Majid, Y. Liu et al., Metallic nanoparticle-carbon nanotube composites for electrochemical determination of explosive nitroaromatic compounds. Anal. Chem. **78**, 5504–5512 (2006)
37. K.K. Kartha, S.S. Babu, S. Srinivasan et al., Attogram sensing of trinitrotoluene with a self-assembled molecular gelator. J. Am. Chem. Soc. **134**, 4834–4841 (2012)
38. C.M. Gonzalez, M. Iqbal, M. Dasog et al., Detection of high-energy compounds using photoluminescent silicon nanocrystal paper based sensors. Nanoscale **6**, 2608–2612 (2014)

39. J.P. Vigneron, J.M. Pasteels, D.M. Windsor et al., Switchable reflector in the Panamanian tortoise beetle Charidotella egregia (Chrysomelidae: Cassidinae). Phys. Rev. E Stat. Nonlinear Soft Matter Phys. **76**, 031907 (2007)
40. R.E. Young, F.M. Mencher, Bioluminescence in mesopelagic squid: diel color change during counterillumination. Science **208**, 1286–1288 (1980)
41. K.S. Bejoymohandas, T.M. George, S. Bhattacharya et al., AIPE-active green phosphorescent iridium(III) complex impregnated test strips for the vapor-phase detection of 2,4,6-trinitrotoluene (TNT). J. Mater. Chem. C **2**, 515–523 (2014)
42. J.W. Oh, W.J. Chung, K. Heo et al., Biomimetic virus-based colourimetric sensors. Nat. Commun. (2014). doi:10.1038/ncomms4043
43. H. Sohn, M.J. Sailor, D. Magde et al., Detection of nitroaromatic explosives based on photoluminescent polymers containing metalloles. J. Am. Chem. Soc. **125**, 3821–3830 (2003)
44. S. Anitha, B. Brabu, T.D. John et al., Optical, bactericidal and water repellent properties of electrospun nano-composite membranes of cellulose acetate and ZnO. Carbohydr. Polym. **87**, 1065–1072 (2012)
45. S. Anitha, T.S. Natarajan, Fabrication of hierarchical ZnO enriched fibrous PVA membrane. J. Nanosci. Nanotechnol. **12**, 1–9 (2012)
46. S. Anitha, B. Brabu, T.D. John et al., Preparation of free-standing electrospun composite ZnO membrane for antibacterial applications. Adv. Sci. Lett. **4**, 1–7 (2012)
47. T. Uyar, J. Hacaloglu, F. Besenbacher, Electrospun polyethylene oxide (PEO) nanofibers containing cyclodextrin inclusion complex. J. Nanosci. Nanotechnol. **11**(5), 3949–3958 (2011)
48. T. Uyar, R. Havelund, J. Hacaloglu et al., Functional electrospun polystyrene nanofibers incorporating alpha, beta and gamma cyclodextrins: comparison of molecular filter performance. ACS Nano **4**(9), 5121–5130 (2010)
49. F. Kayaci, T. Uyar, Electrospun zein nanofibers incorporating cyclodextrins. Carbohydr. Polym. **90**, 558–568 (2012)
50. A. Celebioglu, T. Uyar, Green and one-step synthesis of gold nanoparticles incorporated in electrospun cyclodextrin nanofibers. RSC Adv. **3**, 10197–10201 (2013)
51. A. Celebioglu, O.C.O. Umu, T. Tekinay et al., Antibacterial electrospun nanofibers from triclosan/cyclodextrin inclusion complexes. Colloids Surf. B **116**, 612–619 (2014)
52. Y. Che, D.E. Gross, H. Huang et al., Diffusion-controlled detection of trinitrotoluene: interior nanoporous structure and low highest occupied molecular orbital level of building blocks enhance selectivity and sensitivity. J. Am. Chem. Soc. **134**, 4978–4982 (2012)
53. F. Wang, W. Wang, B. Liu et al., Copolypeptide-doped polyaniline nanofibers for electrochemical detection of ultra trace trinitrotoluene. Talanta **79**, 376–382 (2009)
54. Y. Wang, A. La, Y. Ding et al., Novel signal-amplifying fluorescent nanofibers for naked-eye-based ultrasensitive detection of buried explosives and explosive vapors. Adv. Funct. Mater. **22**, 3547–355 (2012)
55. J.H. Lee, S. Kang, J.Y. Lee et al., Instant visual detection of picogram levels of trinitrotoluene by using luminescent metal–organic framework gel-coated filter paper. Chem. Eur. J. **19**, 16665–16671 (2013)
56. H. Xu, F. Liu, Y. Cui et al., A luminescent nanoscale metal–organic framework for sensing of nitroaromatic explosives. Chem. Commun. **47**, 3153–3155 (2011)
57. Y. Xu, Y. Wen, W. Zhu et al., Electrospun nanofibrous mats as skeletons to produce MOF membranes for the detection of explosives. Mater. Lett. **87**, 20–23 (2012)
58. Y. Yang, H. Wang, K. Su et al., A facile and sensitive fluorescent sensor using electrospun nanofibrous film for nitroaromatic explosive detection. J. Mater. Chem. **21**, 11895 (2011)
59. Y.Y. Lv, W. Xu, F.W. Lin et al., Electrospun nanofibers of porphyrinated polyimide for the ultra-sensitive detection of trace TNT. Sensor Actuators B Chem. **184**, 205–211 (2013)
60. Y. Long, H. Chen, Y. Yang et al., Electrospun nanofibrous film doped with a conjugated polymer for DNT fluorescence sensor. Macromolecules **42**, 6501–6509 (2009)
61. Y.Z. Liao, V. Strong, Y. Wang et al., Oligotriphenylene nanofiber sensors for detection of nitro-based explosives. Adv. Funct. Mater. **22**, 726–735 (2012)

62. S. Tao, G. Li, J. Yin, Fluorescent nanofibrous membranes for trace detection of TNT vapor. J. Mater. Chem. **17**, 2730–2736 (2007)
63. S. Anitha, C. Asli, U. Tamer, Ultrafast on-site selective visual detection of TNT at sub ppt level using fluorescent gold cluster incorporated single nanofiber. Chem. Commun. (2014). doi:10.1039/C4CC01190B
64. W. Li, N.D. Ho, Y. Cho et al., Nanofibers of conducting polyaniline for aromatic organic compound sensor. Sensor Actuators B-Chem. **143**, 132–138 (2009)
65. C. Deng, P. Gong, Q. He et al., Highly fluorescent TPA-PBPV nanofibers with amplified sensory response to TNT. Chem. Phys. Lett. **483**, 219–223 (2009)
66. W.E. Lee, C.J. Oh, I.K. Kang et al., Diphenylacetylene polymer nanofiber mats fabricated by freeze drying: preparation and application for explosive sensors. Macromol. Chem. Phys. **211**, 1900–1908 (2010)